Available online at www.sciencedirect.com
SCIENCE DIRECT
Composite Structures 75 (2006) 587–592
COMPOSITE STRUCTURES
www.elsevier.com/locate/compstruct

Interlayer stress in laminate beam of piezoelectric and elastic materials

Qing-Sheng Yang [a,*], Qing-Hua Qin [b], Tong Liu [a]

[a] Department of Engineering Mechanics, Beijing University of Technology, Beijing 100022, China
[b] Department of Engineering, The Australian National University, Canberra, ACT 0200, Australia

Available online 24 May 2006

Abstract

This paper studies interfacial mechanical behavior of laminate beams, consisting of two piezoelectric facial sheets and an elastic core. The study is based on coupled multi-filed finite element formulation. The emphasis is placed on mechanical and electric behavior of interfaces between piezoelectric material and elastic material, including effect of geometrical parameters, stress distribution and stress concentration near free edge of the beam subjected to coupling electric and mechanical loads. In particular, various parametric effect of laminate beam is explored and some conclusions are presented which may be useful for designing laminate beam and minimizing stress concentration at the free edges of the beam.

Keywords: Interlayer stress; Laminate; Piezoelectric material; Stress concentration

1. Introduction

Piezoelectric composites have wide application in smart devices and adaptive structures [1]. Since piezoelectric materials usually behaviour brittle failure, fracture analysis of such smart structures is important for their reliability and effective serves [2,3]. For a laminated structure with two piezoelectric cover sheets and an elastic core, the delamination between piezoelectric sheet and the elastic core is a major failure mechanism. Principally, the delamination of the laminated structures is induced by the interlayer stresses of which there are often relatively high concentrations. It is well-known that the concentration of the interlayer stresses usually happens near the free edges of a structure. It should also be mentioned that the interlayer stress level and concentration depend strongly on the geometrical parameters of the structures and properties of the component materials.

Interlayer stresses and the effect of their concentration on mechanical performance have been investigated by many researchers and scientists. Early studies were focused mainly on laminated composite structures. Comprehensive reviews on developments in this field can be found in [4,5]. During the past two decades, the interlayer stresses and failure mechanism of adaptive structures have caused increasingly attention of practical engineers and professional researchers. Due to the difficulty in obtaining theoretical solution for such a complex problem, the finite element method (FEM) is usually employed to model and simulate stress transfer and failure process of interface between layers of the adaptive structures [6–10]. The numerical studies in [6–10] include applications of FEM to piezoelectric laminate beams, plates and shells consisting of piezoelectric sheets and elastic material core. Reports in [11–14] on electro-elastic coupling analyses of piezoelectric structures should also be mentioned.

It is recognized that an excellent design on adaptive structures depends on good understanding of the dependence of structural performance on the loading and structural parameters. Based on this understanding, present work develops an application of 3D FE algorithm to the analysis of interlayer stresses in laminate beams which consists of two piezoelectric cover sheets and an elastic material core. The major emphasis is placed on the interlayer

* Corresponding author.
E-mail addresses: qsyang@bjut.edu.cn (Q.-S. Yang), qinghua.qin@anu.edu.au (Q.-H. Qin).

0263-8223/$ - see front matter © 2006 Elsevier Ltd. All rights reserved.
doi:10.1016/j.compstruct.2006.04.024

stress concentration near free edges and the effect of geometrical parameters and material properties on the interlayer stresses in piezoelectric laminate beams.

2. Basic equations and variational formulation

2.1. Basic equations

Consider a laminate cantilever beam with an elastic core and two piezoelectric sheets (see Fig. 1). It is assumed that the two piezoelectric sheets have the same thickness and therefore only half of the structure is required to be analyzed due to its symmetry. It is noted that, when the piezoelectric sheets extend or contract under external electric loading, the laminated beam will be bended and thus behaviors as an actuator.

For the structure as shown in Fig. 1, the governing equations of mechanical and electric fields are as follows:

Stress equilibrium equations:

$$\sigma_{ij,j} + f_i = 0 \tag{1}$$

Maxwell's equations

$$D_{i,i} = q_b \tag{2}$$

Strain–displacement relations

$$\varepsilon_{ij} = \frac{1}{2}(u_{i,j} + u_{j,i}) \tag{3}$$

Electric field-potential relations

$$E_i = -\phi_i \tag{4}$$

In these equations, σ_{ij} and ε_{ij} are respectively the stress and infinitesimal strain tensors, u_i is the mechanical displacement vector, f_i is the mechanical body force, E_i and D_i are the electric intensity and electric displacement vectors, ϕ is the electric potential, and q_b is the body charge density.

Eqs. (1) and (3) are coupled to Eqs. (2) and (4) through the constitutive equations. For the linear piezoelectric materials, the constitutive relations read

$$\sigma_{ij} = C_{ijkl}\varepsilon_{ij} - e_{ijn}E_n \tag{5}$$

$$D_m = e_{klm}\varepsilon_{kl} + \kappa_{mn}E_n \tag{6}$$

where C_{ijkl} are the elastic stiffness coefficients at constant electric field, e_{ijk} are the piezoelectric stress constants, and κ_{mn} are dielectric permittivities at constant strain.

For elastic core materials, by letting the electric fields vanish, i.e., $\phi = D_i = E_i = 0$, and setting $e_{ijk} = 0$, the constitutive Eqs. (5) and (6) reduce to the Hook's law:

$$\sigma_{ij} = C_{ijkl}\varepsilon_{kl} \tag{7}$$

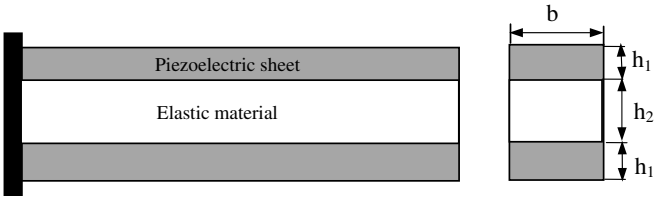

Fig. 1. Laminate beam of piezoelectric and elastic materials.

For the boundary value problem as shown in Fig. 1, Eqs. (1)–(7) are completed by adding the following boundary conditions

$$u_i = \bar{u}_i \quad \text{on } S_u \tag{8}$$

$$t_i = \sigma_{ij}n_j \quad \text{on } S_t \tag{9}$$

$$D_n = D_i n_i = -q_s \quad \text{on } S_D \tag{10}$$

$$\phi = \bar{\phi} \quad \text{on } S_\phi \tag{11}$$

where $\bar{u}_i$, $\bar{t}_i$, $\bar{q}_n$ and $\bar{\phi}$ are, respectively, prescribed boundary displacement, traction vector, surface charge and electric potential, an overhead bar denotes prescribed value, $S = S_u + S_t = S_D + S_\phi$ is the boundary of the solution domain Ω.

2.2. Variational formulation for FE analysis

Based on weighted residual method and the boundary value statement (1)–(11) for the model as shown in Fig. 1, we now present a variational formulation for the purpose of deriving FE stiffness equation. If denote the virtual displacement by δu_i and the virtual electric potential by $\delta\phi$, the equivalent variational statement of the differential equations and boundary conditions (1)–(11) can be written as below:

$$\delta\Pi = \int_V [(\sigma_{ij,j} + f_i)\delta u_i + (D_{i,i} + q_b)\delta\phi]\mathrm{d}V - \int_S [(\sigma_{ij}n_j - t_i)\delta u_i + (D_i n_i + q_s)\delta\phi]\mathrm{d}S = 0 \tag{12}$$

Integrating by parts, we have

$$\delta\Pi = \int_V (\sigma_{ij}\delta u_{i,j} - D_i\delta\phi_{,i})\mathrm{d}V + \int_V (f_i\delta u_i + q_b\delta\phi)\mathrm{d}V + \int_S (t_i\delta u_i - q_s\delta\phi)\mathrm{d}S = 0 \tag{13}$$

Substituting Eqs. (3) and (4) into Eq. (13), one obtains

$$\delta\Pi = \int_V (\sigma_{ij}\delta\varepsilon_{ij} - D_i\delta E_i)\mathrm{d}V - \int_V (f_i\delta u_i + q_b\delta\phi)\mathrm{d}V - \int_S (t_i\delta u_i - q_s\delta\phi)\mathrm{d}S = 0 \tag{14}$$

Using constitutive Eqs. (5) and (6), Eq. (14) becomes

$$\delta\Pi = \int_V [(C_{ijkl}\varepsilon_{kl} - e_{ijn}E_n)\delta\varepsilon_{ij} - (e_{klm}\varepsilon_{kl} + \kappa_{mn}E_n)\delta E_i]\mathrm{d}V - \int_V (f_i\delta u_i + q_b\delta\phi)\mathrm{d}V - \int_S (t_i\delta u_i - q_s\delta\phi)\mathrm{d}S = 0 \tag{15}$$

The variational Eq. (15) can be used to establish the FE equation. For this purpose, the displacement and electric potential are interpolated in the forms

$$\mathbf{u} = \sum_{i=1}^{n} \mathbf{N}_i\mathbf{u}_i = \mathbf{N}\mathbf{u}^e, \quad \boldsymbol{\varepsilon} = \mathbf{L}\mathbf{N}\mathbf{u}^e = \mathbf{B}\mathbf{u}^e \tag{16}$$

$$\phi = \sum_{i=1}^{n} \overline{N}_i\phi_i = \overline{\mathbf{N}}\boldsymbol{\varphi}^e, \quad E_i = -\sum_{i=1}^{n} \overline{N}_{i,i}\phi_i = -\overline{\mathbf{B}}\boldsymbol{\varphi}^e \tag{17}$$

Then Eq. (15) can be rewritten as

$$\begin{aligned}\delta\Pi &= \sum_e \delta\Pi^e \\ &= \sum_e \left\{ \int_{V^e} \left[\delta \mathbf{u}^{e\mathrm{T}} \mathbf{B}^{\mathrm{T}} (\mathbf{C}\mathbf{B}\mathbf{u}^e + \mathbf{e}^{\mathrm{T}} \overline{\mathbf{B}} \boldsymbol{\varphi}^e) + \delta \boldsymbol{\varphi}^{e\mathrm{T}} \overline{\mathbf{B}}^{\mathrm{T}} (\mathbf{e}\mathbf{B}\mathbf{u}^e - \boldsymbol{\kappa} \overline{\mathbf{B}} \boldsymbol{\varphi}^e) \right] \mathrm{d}V \right. \\ &\quad \left. - \int_{V^e} (\delta \mathbf{u}^{e\mathrm{T}} \mathbf{N}^{\mathrm{T}} \mathbf{f} + \delta \boldsymbol{\varphi}^{e\mathrm{T}} \overline{\mathbf{N}}^{\mathrm{T}} q_b) \mathrm{d}V - \int_{S^e} (\delta \mathbf{u}^{e\mathrm{T}} \mathbf{N}^{\mathrm{T}} \mathbf{t} - \delta \boldsymbol{\varphi}^{e\mathrm{T}} \overline{\mathbf{N}}^{\mathrm{T}} q_s) \mathrm{d}S \right\} \\ &= 0 \end{aligned} \tag{18}$$

where $\mathbf{u}^e$, $\boldsymbol{\varphi}^e$ are independent variables. The arbitrariness of $\delta\mathbf{u}^{e\mathrm{T}}, \delta\boldsymbol{\varphi}^{e\mathrm{T}}$ leads to

$$\sum_e \left\{ \int_{V^e} [\mathbf{B}^{\mathrm{T}} \mathbf{C}\mathbf{B}\mathbf{u}^e + \mathbf{B}^{\mathrm{T}} \mathbf{e}^{\mathrm{T}} \overline{\mathbf{B}} \boldsymbol{\varphi}^e] \mathrm{d}V - \int_{V^e} \mathbf{N}^{\mathrm{T}} \mathbf{f} \mathrm{d}V - \int_{S^e} \mathbf{N}^{\mathrm{T}} \mathbf{t} \mathrm{d}S \right\} = 0 \tag{19}$$

$$\sum_e \left\{ \int_{V^e} [\overline{\mathbf{B}}^{\mathrm{T}} \mathbf{e}\mathbf{B}\mathbf{u}^e - \overline{\mathbf{B}}^{\mathrm{T}} \boldsymbol{\kappa} \overline{\mathbf{B}} \boldsymbol{\varphi}^e] \mathrm{d}V - \int_{V^e} \overline{\mathbf{N}}^{\mathrm{T}} q_b \mathrm{d}V + \int_{S^e} \overline{\mathbf{N}}^{\mathrm{T}} q_s \mathrm{d}S \right\} = 0 \tag{20}$$

The matrix form of these equations reads

$$\begin{bmatrix} \mathbf{K}_{\mathbf{mm}} & \mathbf{K}_{\mathbf{me}} \\ \mathbf{K}_{\mathbf{me}} & \mathbf{K}_{\mathbf{ee}} \end{bmatrix} \begin{Bmatrix} \mathbf{u} \\ \boldsymbol{\varphi} \end{Bmatrix} = \begin{Bmatrix} \mathbf{F}_1 \\ \mathbf{F}_2 \end{Bmatrix} \tag{21}$$

This is a fully coupled finite element equation with the stiffness coefficient matrices

$$\mathbf{K}_{\mathbf{mm}} = \sum_e \int_{V^e} \mathbf{B}^{\mathrm{T}} \mathbf{C}\mathbf{B} \mathrm{d}V, \quad \mathbf{K}_{\mathbf{ee}} = \sum_e \int_{V^e} \overline{\mathbf{B}}^{\mathrm{T}} \boldsymbol{\kappa} \overline{\mathbf{B}} \mathrm{d}V \tag{22}$$

$$\mathbf{K}_{\mathbf{me}} = \mathbf{K}_{\mathbf{em}}^{\mathbf{T}} = \sum_e \int_{V^e} \mathbf{B}^{\mathrm{T}} \mathbf{e}^{\mathrm{T}} \overline{\mathbf{B}} \mathrm{d}V \tag{23}$$

$$\begin{aligned} \mathbf{F}_1 &= \sum_e \int_{V^e} \mathbf{N}^{\mathrm{T}} \mathbf{f} \mathrm{d}V + \sum_e \int_{S^e} \mathbf{N}^{\mathrm{T}} \mathbf{t} \mathrm{d}S, \\ \mathbf{F}_2 &= \sum_e \int_{V^e} \overline{\mathbf{N}}^{\mathrm{T}} q_b \mathrm{d}V - \sum_e \int_{S^e} \overline{\mathbf{N}}^{\mathrm{T}} q_s \mathrm{d}S \end{aligned} \tag{24}$$

3. Interlayer stresses

A three dimensional FE model is constructed for analyzing interlayer stresses of laminated beam with two piezoelectric cover sheets and one elastic core. In all calculations, a hexahedral solid element with eight nodes is used to predict interlayer stresses. For the elastic material, there are 3 degrees of freedom (three displacements) at each node, while for piezoelectric sheets, four degrees of freedom (three displacements and one electric potential) are arranged at each node. It is assumed that the length of beam is $l = 20$ mm, the wideness is $b = 4$ mm, the height of the beam cross section is $2h_1 + h_2 = 4.2$ mm. Here the ratio $h_1{:}h_2$ is variable. The used FE mesh is shown in Fig. 2.

The material properties used in the present study are Young's modulus $E = 70$ GPa, Poisson's ratio $\mu = 0.3$ for the elastic material. The properties of piezoelectric materials are $E = 66$ GPa and $\mu = 0.3$. The dielectric constant is $\kappa = 6.145 \times 10^{-5}$ C/Vm and the matrix of piezoelectric stress constants is

$$[e] = \begin{bmatrix} 0 & -512 & 0 \\ 0 & -512 & 0 \\ 0 & 1511 & 0 \\ 1217 & 0 & 0 \\ 0 & 0 & 1217 \\ 0 & 0 & 0 \end{bmatrix} \mathrm{C/m^2}$$

The piezoelectric sheets are so arranged in a way that they have opposite polarization directions (see Fig. 3). That is the polarization of upper sheet is in the positive y-direction and polarization of lower one is along negative y-direction (Fig. 3).

To study the effect of thickness ratio $h_1{:}h_2$ on structural performance, let us consider following three models, e.g. model 1 with $h_1{:}h_2 = 1{:}1$, model 2 with $h_1{:}h_2 = 1{:}5$ and model 3 with $h_1{:}h_2 = 1{:}8$. The three models can cover the

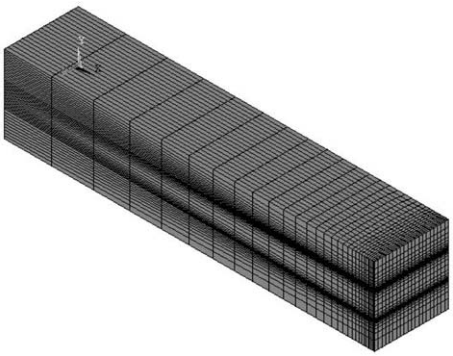

Fig. 2. 3D FE mesh.

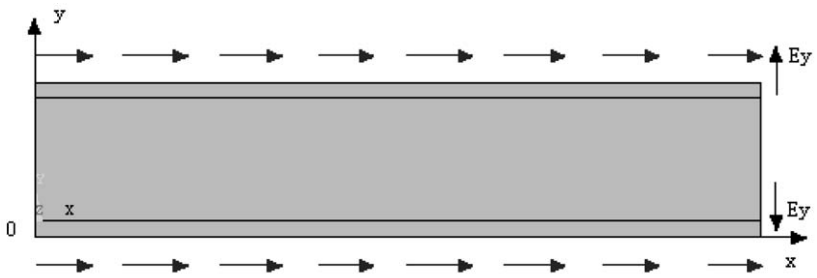

Fig. 3. Polarization of piezoelectric sheets.

most possible thickness ratios for the adaptive structures in practical engineering.

It is well-known that one of the advantages of such adaptive structures is its large actuating force. Therefore, our focus here is on investigating interlayer stresses when the beam acts as an actuator. In this case, the only external load is an electric load applied on the piezoelectric sheets. In our analysis, a voltage with magnitude of 200 V is applied on the external surface of the upper and lower sheets, and the internal surfaces of piezoelectric sheets bonding to elastic material keep zero electric voltage on the interface. Thus the electric fields with opposite directions are formed (Fig. 3).

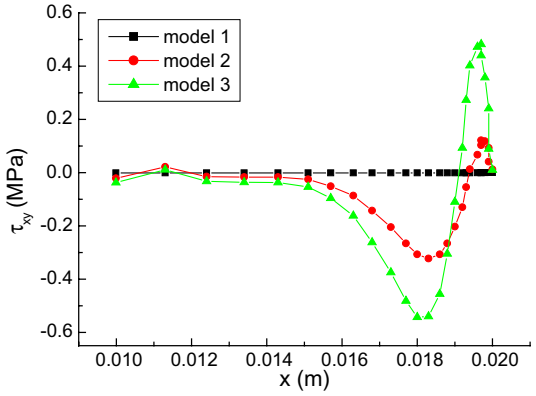

Fig. 5. Variation of interlayer shear stress.

4. Numerical results and discussions

Due to the symmetry of the problem, only lower half of the laminate beam is analyzed. Fig. 4 provides interlayer normal stresses for different models. It can be seen that an extensile stress perpendicular to the interface is induced when the piezoelectric sheets are subjected to the electric load. This normal stress tends to contribute to the delamination of laminate beam and rapidly increases near the free edge. The tress levels and concentrations depend on the thickness ratio of piezoelectric and elastic sheets. For larger thickness ratio, e.g. model 1, the level and concentration of interlayer stress have relative small value. When the thickness of elastic material increases the interlayer stress level and concentration increase dramatically.

Fig. 5 shows distribution of interlayer shear stress along the length of the beam. When it is far from free edge, the shear stress is very small and could be ignored. The obvious oscillation of shear stress appears near free edge. However, the zero shear stress at the free edge is reproduced according to the reciprocate principle of shear stress on two sections with right angle. The shear stress increases as the thickness of piezoelectric sheet decreases. Therefore, it is evident from Figs. 4 and 5 that the interlayer stress is smaller for small value of thickness of the piezoelectric sheets, and the stress level and concentration increase as the thickness of piezoelectric sheet deceases. For this reason, the beam with small thickness of piezoelectric sheet and large thickness of elastic material will be delaminated easily.

To explore distribution of bending stress along the height of the beam, a cross-section is taken at the half length of the beam and the corresponding numerical results are presented in Fig. 6 which exhibits distribution of the bending stress along the height of the cross-section for different models. It is found from Fig. 6 that there is a linear distribution of bending stress along the height of the cross-section. It is also noted that for relatively thick elastic layers, e.g. model 2 and model 3, the bending stresses in the elastic layers are symmetric about neutral axis, while the bending stresses in the two piezoelectric sheets are in opposite sign, one is in extensile and another is in compressive. A bigger jump of bending stresses at the interface is observed. However, for the case of thin elastic layer, the stress in each piezoelectric sheet varies from a compress stress to an extensile stress. The bending stresses in piezoelectric sheets are the actuating forces of the adaptive beam. The comparison of different cases in Fig. 6 illustrates the relative large actuating force can be obtained for the thinner piezoelectric sheets.

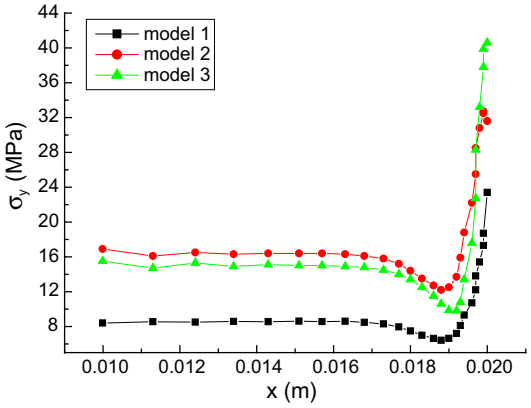

Fig. 4. Variation of interlayer normal stress.

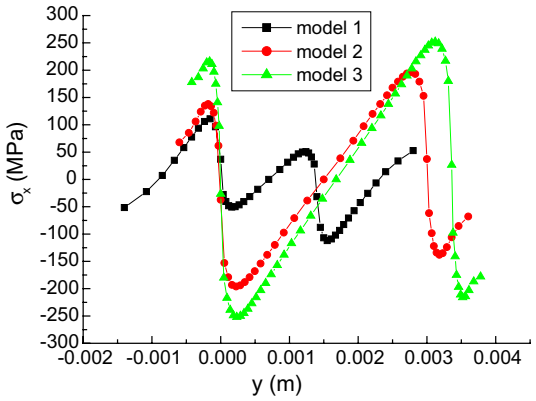

Fig. 6. Bending stress distributions along height of section.

The effect of material properties on the interlayer stress is investigated below. Since the choice of piezoelectric material is very limited, The change in the properties of elastic material is considered in the present study. Here three sets of properties of elastic materials are selected, i.e., material 1: $E = 70$ GPa, $\mu = 0.3$, material 2: $E = 14$ GPa, $\mu = 0.3$, material 3: $E = 25$ GPa, $\mu = 0.3$. For simplicity and conciseness, following discussions are limited to model 1 only, i.e., the model with thickness ratio $h_1{:}h_2 = 1{:}1$.

Fig. 7 shows the influence of properties of elastic materials on interlayer normal stress. It is shown that the properties of the elastic material slightly affect the interlayer normal stress, but dramatically affect the degree of stress concentration near the free edge. The larger stiffness of the elastic material leads to more serious concentration of the interlayer normal stress. This should be taken into account in the design of laminate beam.

Fig. 8 exhibits the influence of properties of the elastic material on the interlayer shear stress where a slight difference can be found for three sorts of elastic materials. The numerical results of interlayer normal and shear stresses for different elastic materials show that the properties of the elastic material affect the normal stress concentration only, although it can slightly affect both the normal stress and shear stress levels.

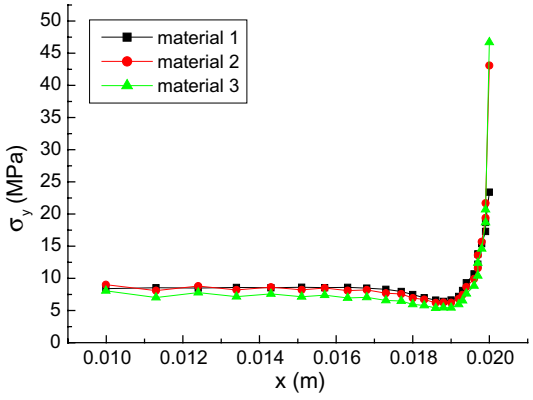

Fig. 7. Influence of properties of elastic materials on interlayer normal stress.

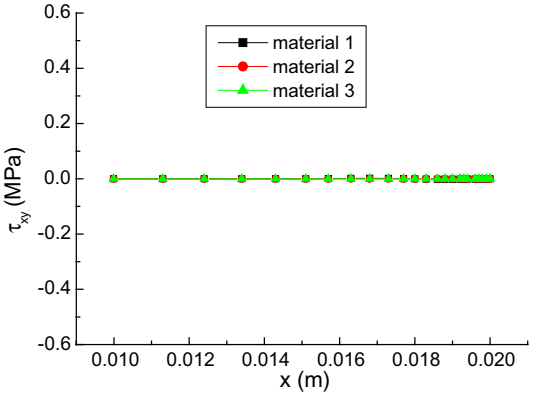

Fig. 8. Influence of properties of elastic materials on interlayer shear stress.

5. Conclusions

Present work studies the interlayer stresses and their concentrations near free edge in laminate beam of piezoelectric and elastic materials by 3D finite element method. The influence of geometrical and material parameters is addressed. Numerical results are obtained and the research conclusions can be summarized as follows:

(1) The interlayer stresses, including normal and shear stress, exist in laminate beam of piezoelectric and elastic materials. There are serious stress concentrations near the free edge of the beam.
(2) The interlayer stress level and concentration depend on the thickness ratio of piezoelectric and elastic layers. The relatively large thickness of the piezoelectric sheet can reduce the interlayer stress level and concentration. But thin piezoelectric sheets often lead to relatively large interlayer stress level and concentration near the free edge of the beam.
(3) The properties of the elastic material slightly affect the interlayer stresses except the normal stress concentration near free edge of the beam.
(4) The bending stress linearly distributes along the section height of the beam. There are bigger jumps in the interfaces between the piezoelectric and elastic materials.

Acknowledgments

The financial support of Natural Science Foundation of China (10272006, 10472082, 30470439) is gratefully acknowledged.

References

[1] Qin QH. Fracture mechanics of piezoelectric materials. Southampton: WIT Press; 2001.
[2] Yu SW, Qin QH. Damage analysis of thermopiezoelectric properties: part I-crack tip singularties. Theore Appl Frac Mech 1996;25:263–77.
[3] Qin QH, Yu SW. An arbitrarily-oriented plane crack terminating at interface between dissimilar piezoelectric materials. Int J Solids Struct 1997;34:581–90.
[4] Kant T, Swaminathan K. Estimation of transverse interlaminar stresses in laminated composites—a selective review and survey of current developments. Compos Struct 2000;49:65–75.
[5] Mittelstedt C, Becker W. Interlaminar stress concentrations in layered structures, Part I: A selective literature survey on the free edge effect since. J Compos Mater 2004;38(12):1037–62.
[6] Chandrashekhara K, Agarwal AN. Active vibration control of laminated composite plates using piezoelectric devices: a finite element approach. J Intel Mater Syst Struct 1993;4:496–508.
[7] Hwang W-S, Park HC. Finite element modeling of piezoelectric sensors and actuators. AIAA J 1993;31(5):930–7.

[8] Ha SK, Keilers C, Chang F-K. Finite element analysis of composite structures containing distributed piezoceramic sensors and actuators. AIAA J 1992;30(3):772–80.
[9] Gopinathan SV, Varadan VV, Varadan VK. A review and critique of theories for piezoelectric laminates. Smart Mater Struct 2000;9(1): 24–48.
[10] Benjeddou A. Advances in piezoelectric finite element modeling of adaptive structural elements: a survey. Comput Struct 2000;76: 347–63.
[11] Lim CW, Lau CWH. A new two-dimensional model for electro-mechanical response of thick laminated piezoelectric actuator. Int J Solid Struct 2005;42:5589–611.
[12] Artel J, Becker W. Coupled and uncoupled analyses of piezoelectric free-edge effect in laminated plates. Compos Struct 2005;69:329–35.
[13] Kapuria S, Achary GGS. A coupled consistent third-order theory for hybrid piezoelectric plates. Compos Struct 2005;70:120–33.
[14] Sze KY, Yang XM, Fan H. Electric assumptions for piezoelectric laminate analysis. Int J Solid Struct 2004;41:2363–82.